UNITED STATES DEPARTMENT OF THE INTERIOR

GEOLOGICAL SURVEY

EFFECT OF SOIL STRUCTURE INTERACTION ON SEISMOGRAMS

by

G. N. Bycroft and P. N. Mork

OPEN-FILE REPORT
83--328

EFFECT OF SOIL STRUCTURE INTERACTION ON SEISMOGRAMS

G. N. Bycroft and P. N. Mork

ABSTRACT

This paper discusses the effect of soil structure interaction on seismograms. In particular, seismograms of the 1979 Imperial Valley earthquake, taken from two instruments located close together, are discussed. One of these instruments is down hole and the other one is housed inside the recorder structure. It is shown that soil structure interaction theory accounts well for the differences in the measured vertical accelerations but not so well for the horizontal accelerations.

INTRODUCTION

Seismometers are used to measure both the three translational components of the free-field ground motion caused by earthquakes and the resulting motions of structures. The free-field ground motion is, strictly, the motion of a point on the ground surface or in the interior unaffected by any structures. It is measured by installing seismometers on concrete pads on the ground surface or down bore holes in selected locations. Buildings are often instrumented by placing seismometers at various levels in the building including one location in the basement. This basement measurement gives the input motion to the structure and is also commonly interpreted as giving the free-field motion at that location.

It has long been recognized however, that the presence of a structure changes the local free-field ground motion. This is because the motion of the structure causes stresses to be exerted on the ground under the structure and these stresses alter the free-field motion. This mechanism is generally referred to as soil-structure interaction. Although, in many cases the interaction is small for certain structures located on a terrain having a low shear-wave velocity, the interaction can be significant for the higher excitation frequencies.

A massless foundation on the ground surface would move with the free-field ground motion. The addition of a structure to the massless foundation will now change this free-field motion due to the stresses generated by the motion of the structure and exerted on the foundation. In every case of seismometer placement for free-field studies, there is an associated structure whether it be the concrete pad and protective shelter used at a "free-field" site or a building basement. In order to determine this interaction effect, it is necessary to determine the compliance functions of a massless rigid plate seated on a suitable model of the ground. These compliance functions express the displacements and rotations of the plate when it is subjected to oscillatory forces and moments. Using these functions, the equations of motion of the structure and the foundation may then be solved to give the interaction motion. This concept has been the basis of all aseismic design using the notion of free-field motion. The compliance functions may be determined experimentally by applying forces and couples to the foundation and measuring its motion. These forces may be oscillatory forces from a vibrator or a simple step function generated by release of a tensioned cable. They may be determined theoretically by treating the ground as an elastic half-space.

Approximate analytical solutions for the compliance functions in one or more of the four degrees of freedom have been given by Reissner (1937), Sung (1953), Bycroft (1956), and Lysmer (1966). Luco and Westmann (1971) and Veletsos and Wei (1971) have provided numerical solutions for an extended frequency range.

For simplicity a circular base is considered. These results may be expressed by using the following notation:

λ, μ = the Lame elastic constants of the elastic half-space   (1)

ρ = density of the elastic half-space (2)

ν = Poisson's ratio of the elastic half-space (3)

p = angular frequency of the impressed forces or couples (4)

The constants h and k are defined by:

$$\frac{\rho p^2}{\mu} = k^2, \frac{\rho p^2}{(\lambda+2\mu)} = h^2$$ (5)

a_0 = kr_0, the non-dimensional frequency factor (6)

r_0 = radius of the plate (7)

U,V,W, = displacements of the center of the plate in the respective coordinate directions when excited by a force P (8)

$$U, V, \text{ or } W = \frac{Pe^{ipt}}{\mu r_0} (f_{1K} + if_{2K})$$ (9)

and

ϕ = the angle of rotation of the plate when excited by a couple M (10)

and

$$\phi = \frac{Me^{ipt}}{\mu r_0^3} (f_{1R} + if_{2R})$$ (11)

where K is V or H for the vertical or horizontal and R refers to the rotational mode. The compliance functions f_{1K} and f_{2K} are functions of a_0 and ν and are different for each of the modes. The function f_2 tends to zero as the frequency tends to zero and the function f_1 then corresponds to the static stiffness of the plate in translation or rotation. For finite frequencies the function f_2 represents energy propagated to infinity and consequently appears as a damping factor. These functions are shown in Figures 1, 2, and 3 for the cases of vertical translation, horizontal translation, and rotation about a

horizontal axis respectively and have been taken from Luco and Westmann (1971). A horizontal force causes a small rotation of the plate as well as horizontal translation, but this will be ignored in the following. The object of this investigation is to use these functions, together with equations of motion of the foundation or relatively rigid housing, to explain differences in seismograms caused by interaction.

Vertical ground motion. The simplest case is of the vertical component of the ground motion. This was treated by Bycroft (1957) and it was shown that the attenuation or magnification R of the ground motion for simple harmonic motion is given by

$$R = \frac{1}{[(1 - b_1 a_0^2 f_1 v)^2 + (b_1 a_0^2 f_2 v)^2]^{1/2}} \qquad (12)$$

where

$$b_1 = \frac{m}{\rho r_0^3} \qquad (13)$$

and

m = mass of the foundation or the rigid housing $\qquad (14)$

Figure 4 shows the function R as a function of a_0.

Horizontal ground motion. In this case both horizontal translation and rotation about a horizontal axis take place. The motions are coupled by the equation of motion of the body.

Let

h_1 = height of center of gravity of the structure above the ground level $\qquad (15)$

h_2 = height of sensing part of seismometer above ground level $\qquad (16)$

I = moment of inertia of the structure about its center of gravity $\qquad (17)$

$$\lambda_1 = \frac{h_1}{r_0} \tag{18}$$

$$\lambda_2 = \frac{h_2}{r_0} \tag{19}$$

$$b_2 = \frac{1}{\rho r_0^5} \tag{20}$$

Bycroft (1978) showed that the ratio R for the sensing point of the installation for this case is given by,

$$R = \frac{[(X^2 + Y^2 + XL + YN)^2 + (XN - YL)^2]^{1/2}}{(X^2 + Y^2)}. \tag{21}$$

where

$$X = 1 - b_2 a_0^2 f_{1R} - b_1 a_0^2 f_{1H} + b_1 b_2 a_0^4 (f_{1H} f_{1R} - f_{2H} f_{2R}) - b_1 a_0^2 \lambda_1^2 f_{1R} \tag{22}$$

$$Y = -b_2 a_0^2 f_{2R} - b_1 a_0^2 f_{2H} + b_1 b_2 a_0^4 (f_{1H} f_{2R} + f_{2H} f_{1R}) - b_1 a_0^2 \lambda_1^2 f_{2R}. \tag{23}$$

$$L = b_1 a_0^2 \lambda_1 \lambda_2 f_{1R} + b_1 a_0^2 [f_{1H} - b_2 a_0^2 f_{1H} f_{1R} + b_2 a_0^2 f_{2H} f_{2R}] \tag{24}$$

$$N = b_1 a_0^2 \lambda_1 \lambda_2 f_{2R} + b_1 a_0^2 [f_{2H} - b_2 a_0^2 f_{1H} f_{2R} - b_2 a_0^2 f_{2H} f_{1R}]. \tag{25}$$

If the free-field motion is given by $Y(t)$ and the measured motion is $Z(t)$ it is readily shown from the Fourier integral theorem that

$$Z\left(\frac{T}{K}\right) = \frac{1}{2\pi} \int_{-\infty}^{+\infty} \overline{Y}(Ka_o) \; H(a_o) e^{ia_o T} \, da_o \tag{26}$$

where

$$\overline{Y}(Ka_o) = \int_{-\infty}^{+\infty} Y\left(\frac{T}{K}\right) e^{-ia_o T} \, dT \tag{27}$$

Vertical case:

$$H = \frac{A + iB}{(A^2 + B^2)} \tag{28}$$

$$A = 1 + ba_o^2 \, f_{1_V} \tag{29}$$

$$\tag{30}$$

$$B = b_1 \, a_o^2 \, f_{2_V}$$

Horizontal and Rocking Case:

$$H = \frac{X^2 + Y^2 + XL + YN + i(XN - YL)}{(X^2 + Y^2)} \tag{31}$$

$$T = Kt \tag{32}$$

$$K = \frac{1}{r_\rho} \sqrt{\frac{\mu}{\rho}} \tag{33}$$

The inverse of equations (26) and (27) give the free-field motion in terms of the measured motion.

If the free-field motion is given by $Y(t)$ and the measured motion is $Z(t)$ it is readily shown from the Fourier integral theorem that

$$Z\left(\frac{T}{K}\right) = \frac{1}{2\pi} \int_{-\infty}^{+\infty} \overline{Y}(Ka_o)\, H\,(a_o)\, e^{ia_o T}\, da_o \tag{26}$$

where

$$\overline{Y}(Ka_o) = \int_{-\infty}^{+\infty} Y\left(\frac{T}{K}\right) e^{-ia_o T}\, dT \tag{27}$$

Vertical case:

$$H = \frac{A + iB}{(A^2 + B^2)} \tag{28}$$

$$A = 1 + ba_o^2\, f_{1_v} \tag{29}$$

$$\tag{30}$$

$$B = b_1\, a_o^2\, f_{2_v}$$

Horizontal and Rocking Case:

$$H = \frac{X^2 + Y^2 + XL + YN + i(XN - YL)}{(X^2 + Y^2)} \tag{31}$$

$$T = Kt \tag{32}$$

$$K = \frac{1}{r_o} \sqrt{\frac{\mu}{\rho}} \tag{33}$$

The inverse of equations (26) and (27) give the free-field motion in terms of the measured motion.

1979 Imperial Valley Earthquake. An array of six DCA instruments was installed over a distance of 305 m in El Centro in time to measure the 1979 Imperial Valley earthquake. An SMA-1 seismograph was also installed in the building housing the recording equipment. This building is an 2.5m cube made out of concrete blocks and located on terrain having a shear wave velocity of 150m/sec for the upper 9m. The building is relatively rigid and fairly heavy and the shearwave velocity of the terrain is low. This situation may well exhibit soil structure interaction effects. Indeed it was noticed that there is a substantial discrepancy between the readings obtained from the SMA-1 instrument located in the recorder building and that of the closest DCA instrument located 1m downhole about 9m away. Estimations show that the down hole DCA should show very small soil structure interaction. Figure 5 shows the vertical component measured as a free-field value by the DCA and Figure 6 shows the vertical component measured inside the building by the SMA-1. The acceleration is cm/sec^2 and the time is seconds. A significant difference is seen in that the amplitude is substantially greater inside the building. A value of $b_1 = 4.5$ and $K = 100$ was calculated for the building and inserted in equations (26) and (27) together with the free-field vertical ground motion from the DCA and evaluated by a Fast Fourier transform procedure. Asymptotic values from Bycroft (1977) were used for the compliance functions for values of a_0 greater than 10. Figure 7 shows that this theoretical building motion compares favorably in amplitude and shape with the measured building motion shown in Figure 6. In the horizontal case much less interaction is to be expected because of the much lower frequency content. Figures 8 and 9 show a difference between the free field DCA horizontal motion and the motion of the building measured by the SMA-1. Figure 10 shows the theoretical motion of the building and although it predicts a certain amplification it does not explain the differences as well as in the vertical case. It appears that some peaks from the DCA have been clipped. It has been suggested that burying the seismometers down hole may account for the difference. A quarter wavelength corresponds to a frequency of 40 Hz and this may be sufficient to clip off the peaks.

CONCLUSIONS

Soil structure interaction theory predicts that the vertical acceleration of the recorder building should be somewhat greater than the free-field motion. This is confirmed by comparing the seismogram from the SMA-1 instrument inside the recorder building with the free-field motion given by the DCA instrument. Further, the calculated vertical acceleration of the building compares favorably with the measured motion. For horizontal accelerations the theory predicts little difference between the free-field accelerations and the acceleration of the building. The theoretical horizontal acceleration compares well with the measured motion in certain regions but not for some peaks where there is evidence of peaks being clipped by the DCA.

REFERENCES

Reissner, E. (1937). Stationare axial symmetrische, durch eine schuttelnde masse erregte schwingungen eines homogen elastichen halbraumes, Ing. Arch. 8, 381-396.

Sung, T.Y. (1953). Vibrations in semi-infinite solids due to periodic surface loading, Am. Soc. Testing Mater. Spec. Tech. Publ. Symp. Dynamic Testing of Soils 156, 35-38.

Bycroft, G.N. (1956). Forced vibrations of a rigid circular plate on a semi-infinite elastic space and on an elastic stratum, Phil. Trans. Roy. Soc. London, Ser. A, 948, 327-368.

Lysmer, J. and F.E. Richart. (1966). Dynamic response of footings to vertical loading, J. Soil Mech. Found. Div., Proc. Am. Soc. Civil Engrs., 92, 65-91.

Luco, J.E. and R.A. Westman (1971). Dynamic response of circular footings, J. Eng. Mech. Div., Proc. Am. Soc. Civil Engrs., 97, 1381-1395.

Veletsos, A.D. and Y.T. Wei (1971). Lateral and rocking vibration of footings, J. Soil Found. Div., Proc. Am. Soc. Civil Engrs., 97, 1227-1248.

Bycroft, G.N. (1957). The magnification caused by partial resonance of the foundation of a ground vibration detector, Trans. Am. Geophys. Union, 38, 928-930.

Bycroft, G.N. (1978). The effect of soil structure on seismometer readings, B.S.S.A., 68, No. 3, June 1978.

Bycroft, G.N. (1977). Soil structure interaction at higher frequency factors, Earthquake Engineering and Structural Dynamics, 5, No. 3.
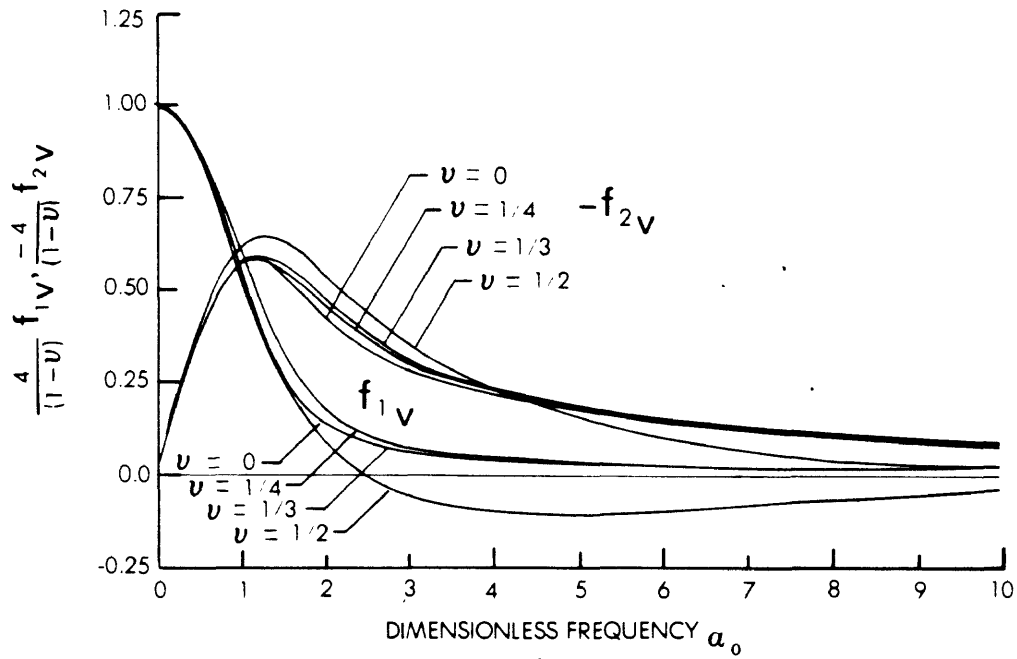
FIGURE CAPTIONS

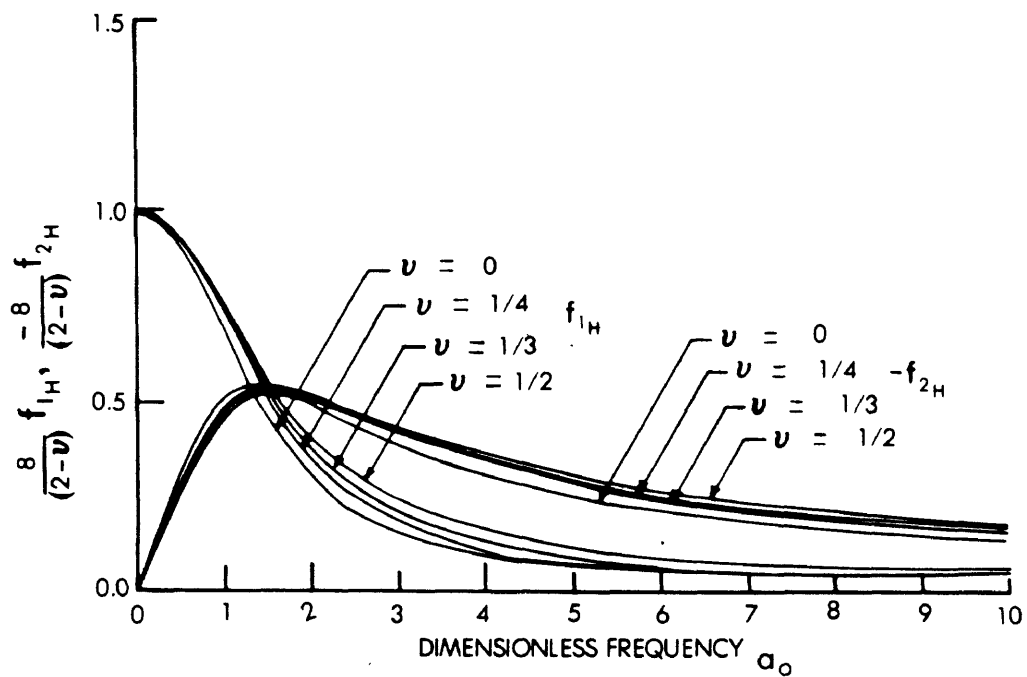Figure 1-- Vertical compliance functions as a function of α_0 and ν.

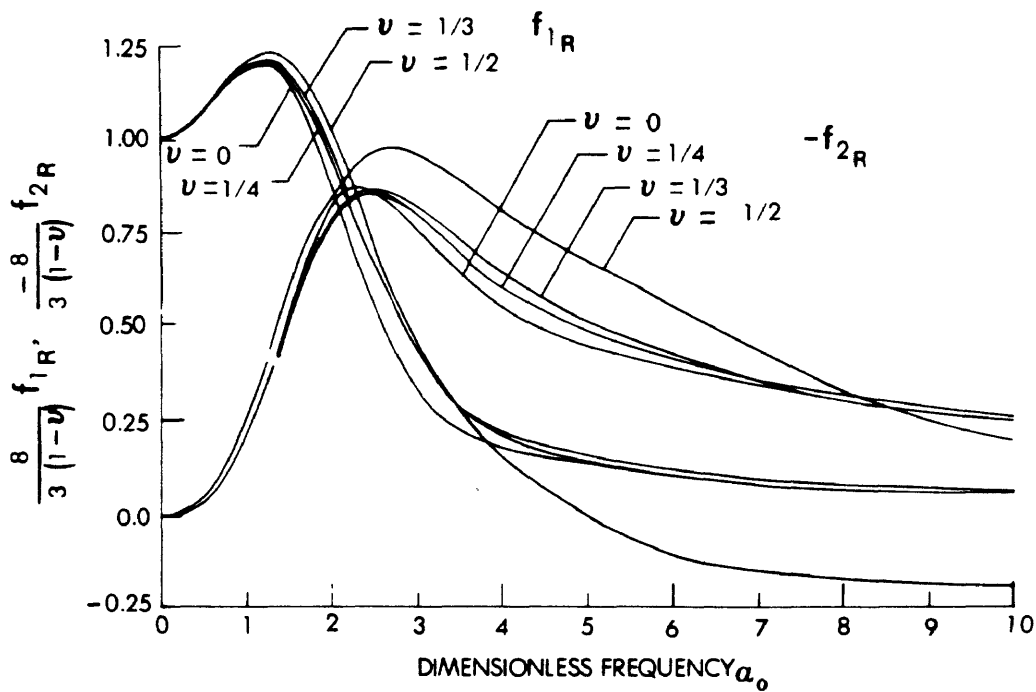Figure 2-- Horizontal compliance functions as a function of α_0 and ν.

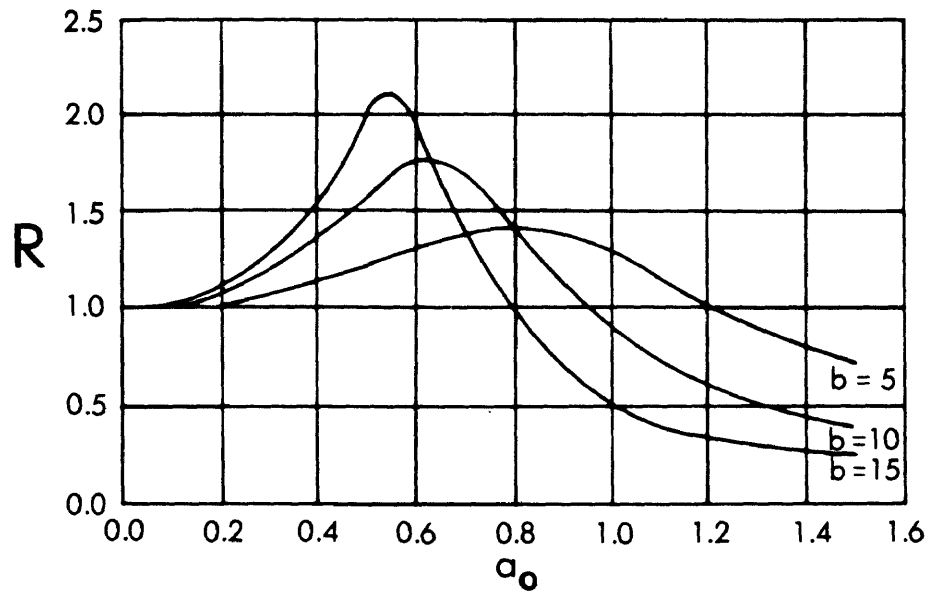Figure 3-- Rotational compliance functions as a function of α_0 and ν.

Figure 4-- Function R as a function of α_0 and b.
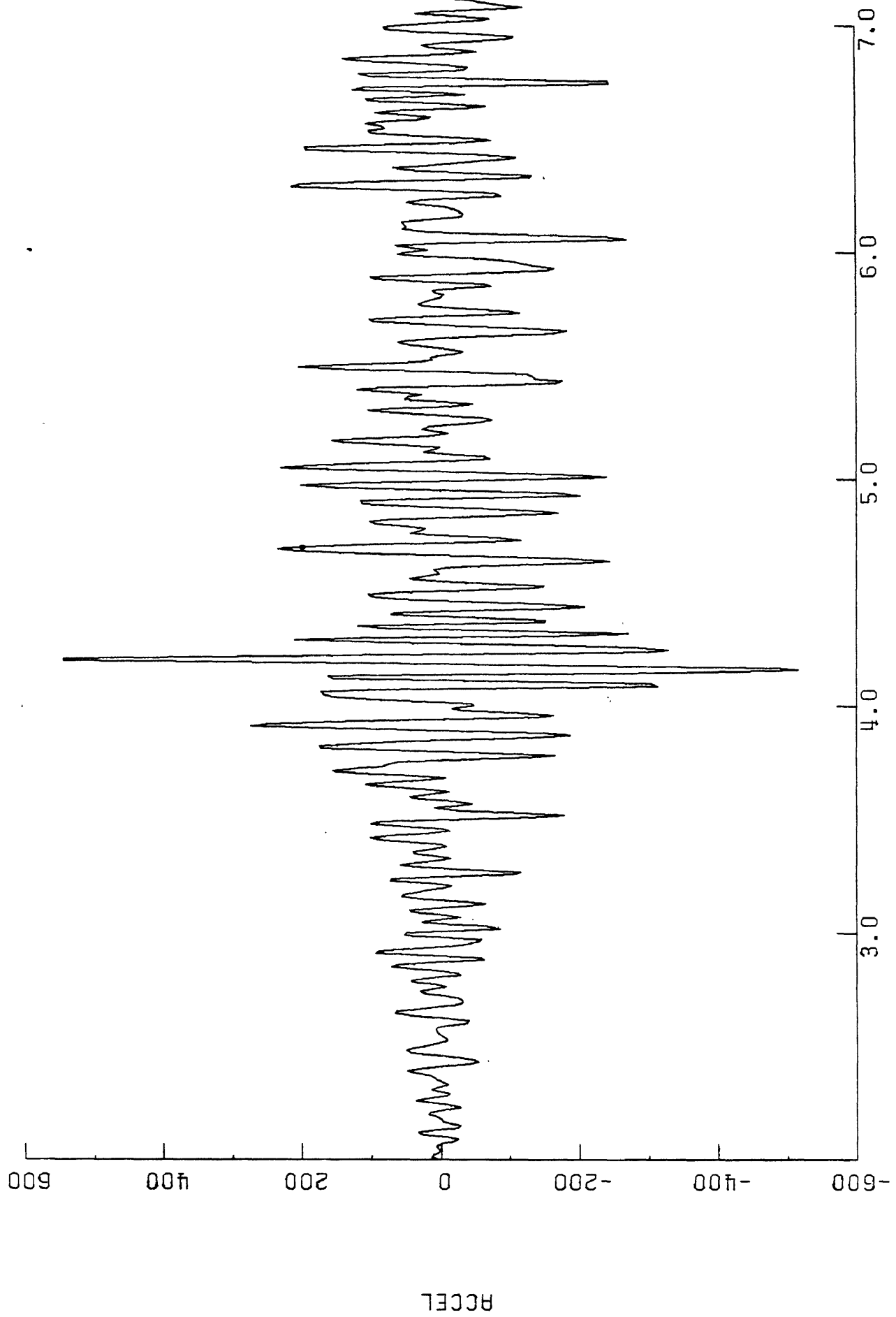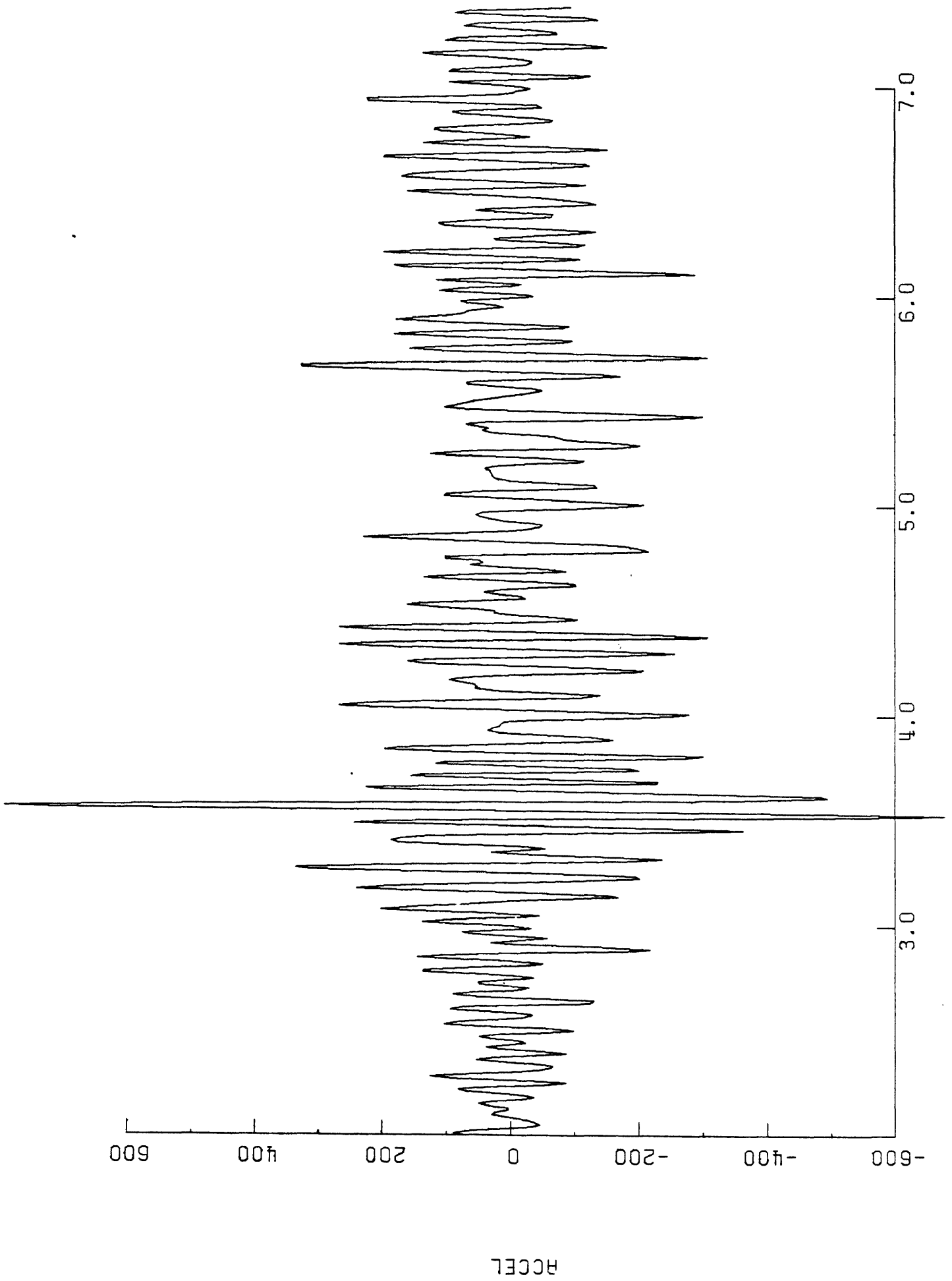
Figure 5-- Vertical component free field DCA.
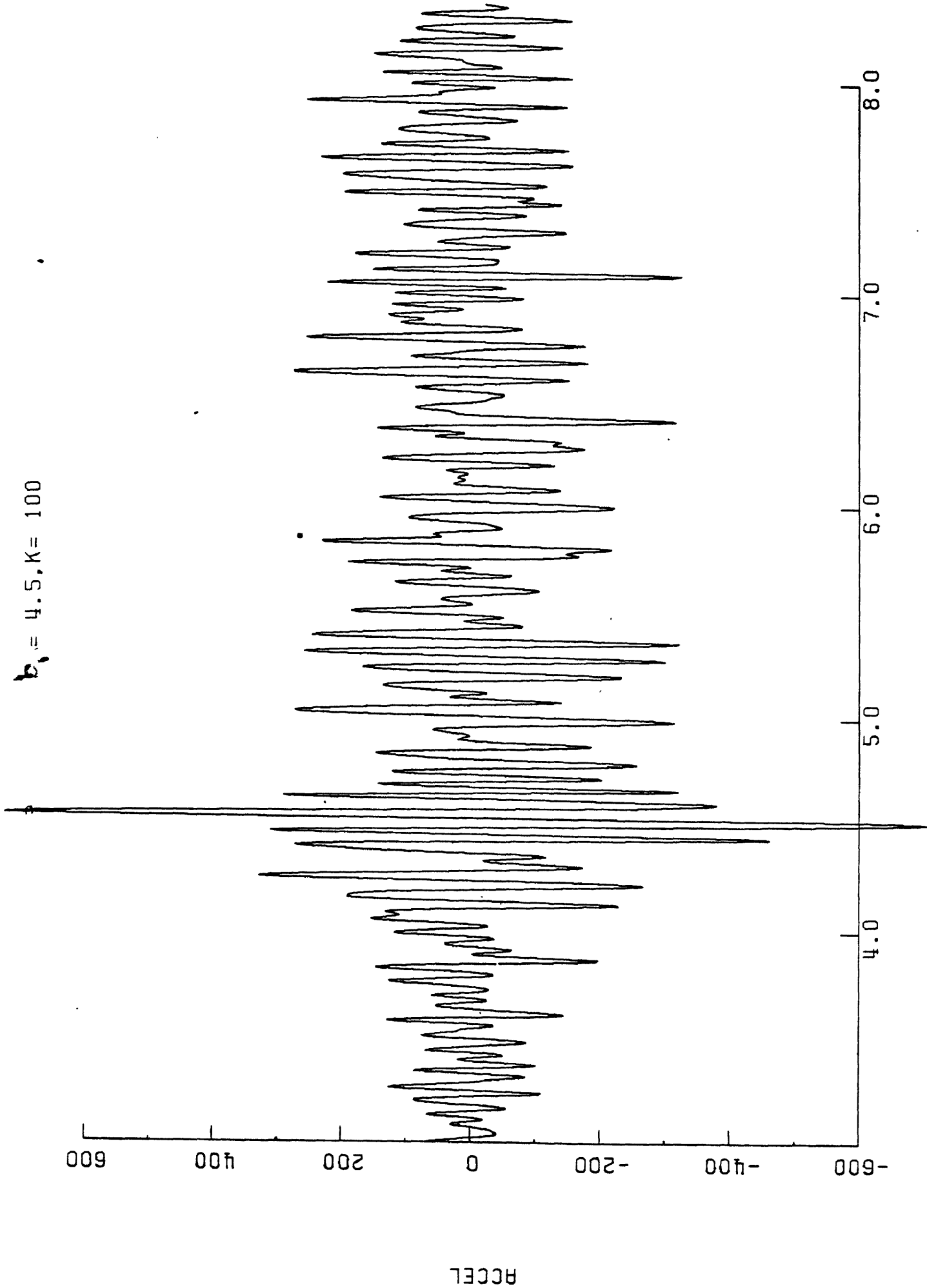
Figure 6-- Building vertical component SMA-1.

Figure 7-- Theoretical vertical component.

Figure 8-- Horizontal component free field DCA.

Figure 9-- Building horizontal component SMA-1.

Figure 10-- Theoretical horizontal building motion.

Figure 1.- Vertical compliance functions as a function of α_0 and ν.

Figure 2.– Horizontal compliance functions as a function of α_0 and ν.

Figure 3.– Rotational compliance functions as a function of α_0 and ν.

Figure 4.- Function R as a function of α_0 and b

Figure 5.- Vertical component free field DCA.
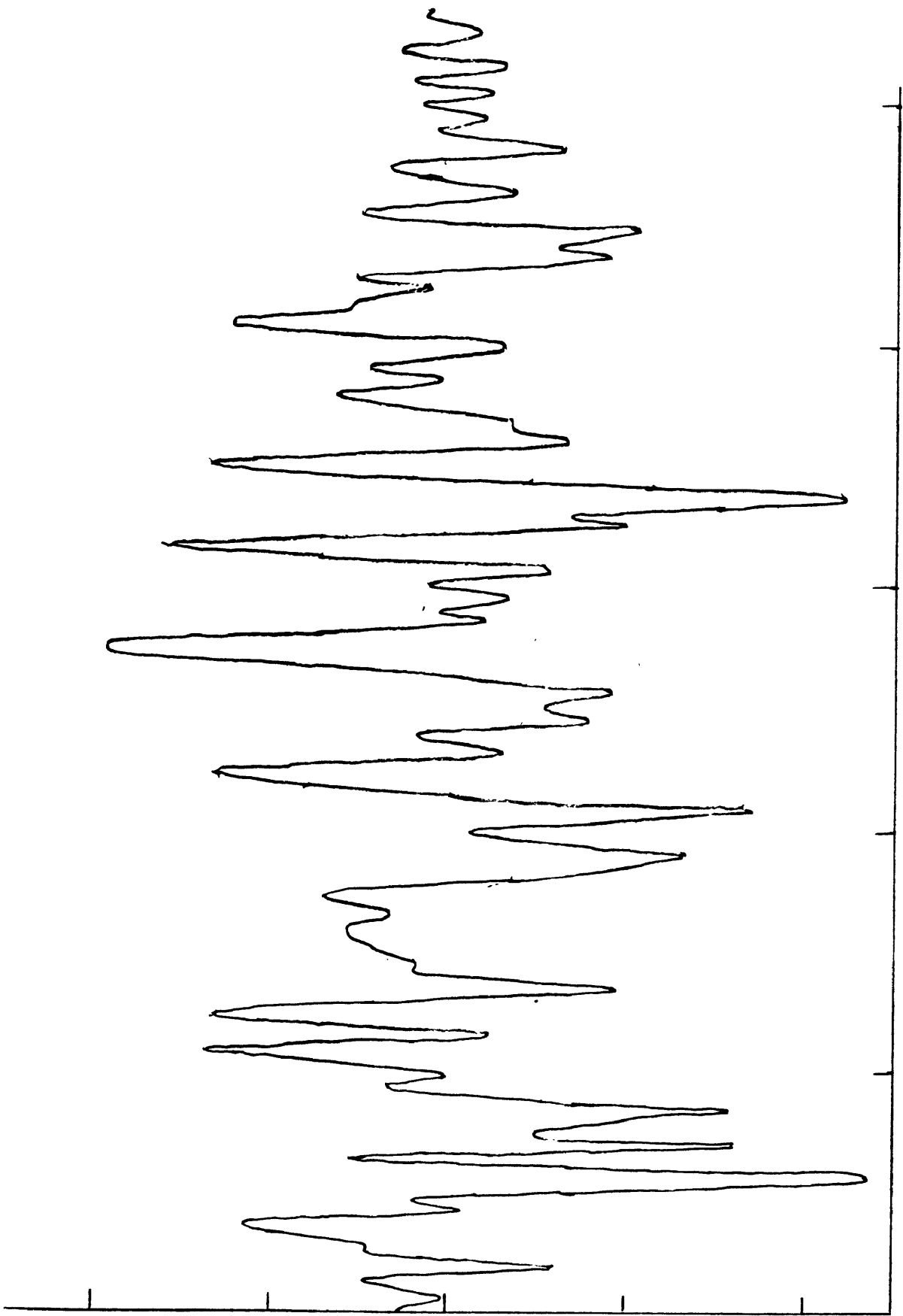
Figure 6.– Building vertical component SMA-1.

Figure 7.- Theoretical vertical component.
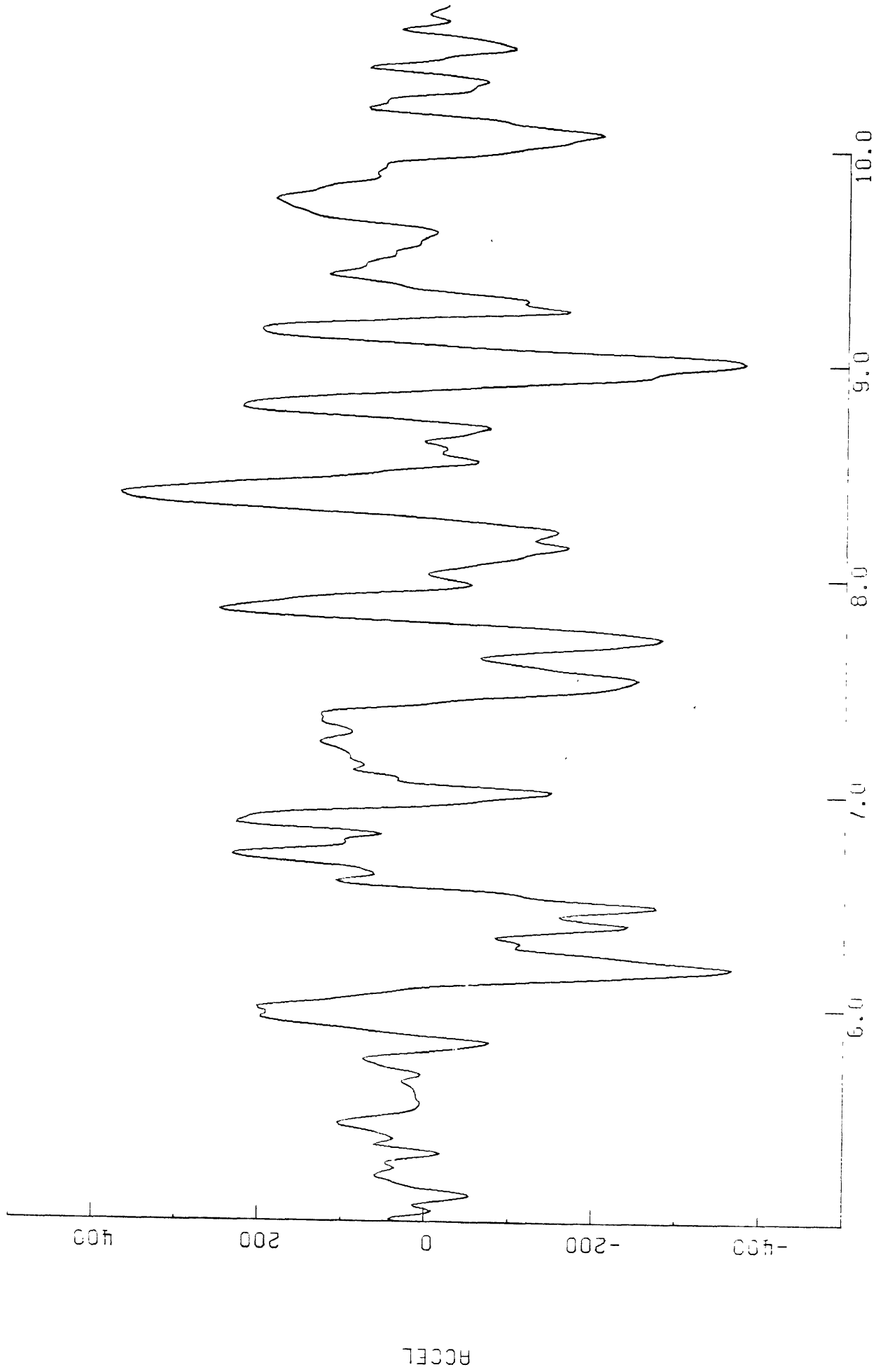
Figure 8. - Horizontal component free-field DCA.

TIME

Fig. 9.- Building horizontal component SMA-1.
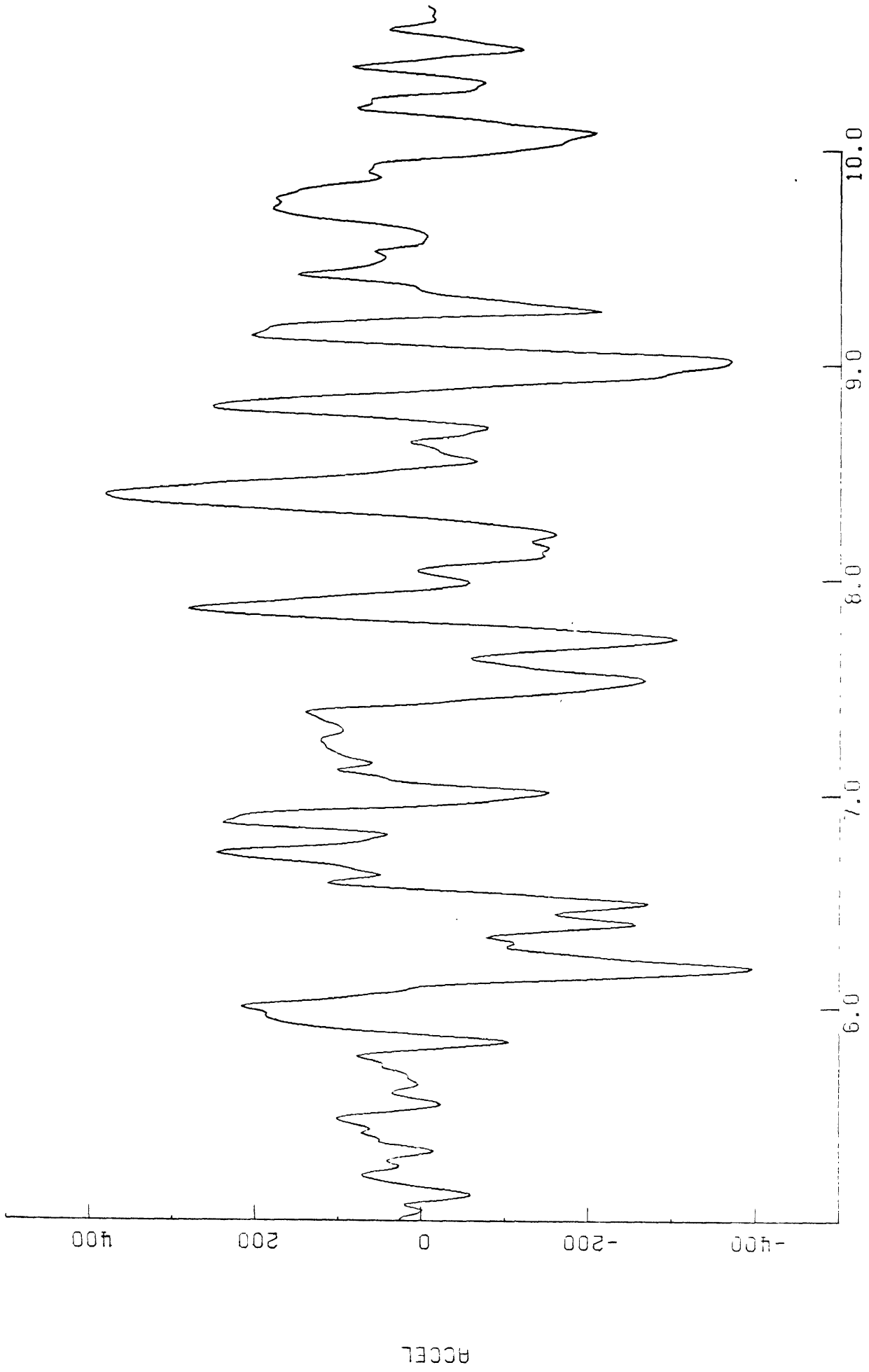
L1=0.89,L2=0.10,K=100,B1=4.5,B2=4.0

ACCEL

TIME

Fig. 10.- Theoretical horizontal building motion.